The pion-photon transition form factor at two loops in QCD

Jing Gao[1,2,3,4], Tobias Huber[2*], Yao Ji[5,2] and Yu-Ming Wang[1]

1 School of Physics, Nankai University, Weijin Road 94, 300071 Tianjin, China
2 Naturwissenschaftlich-Technische Fakultät, Universität Siegen,
Walter-Flex-Str. 3, 57068 Siegen, Germany
3 Institute of High Energy Physics, CAS, P.O. Box 918(4) Beijing 100049, China
4 School of Physics, University of Chinese Academy of Sciences, Beijing 100049, China
5 Physik Department T31, James-Franck-Straße 1, Technische Universität München,
D-85748 Garching, Germany

★ huber@physik.uni-siegen.de

*15th International Symposium on Radiative Corrections:
Applications of Quantum Field Theory to Phenomenology,
FSU, Tallahasse, FL, USA, 17-21 May 2021*

Abstract

We report on the fully analytic calculation of the leading-power contribution to the photon-pion transition form factor $\gamma\gamma^* \to \pi^0$ at two loops in QCD. The applied techniques are based on hard-collinear factorization, together with modern multi-loop methods. We focus both, on the technical details such as the treatment of evanescent operators, and the phenomenological implications. Our results indicate that the two-loop correction is numerically comparable to the one-loop effect in the same kinematic domain. We also demonstrate that our results will play a key role in disentangling various models for the twist-two pion distribution amplitude thanks to the envisaged precision at Belle II.

1 Introduction

Hard exclusive processes play a prominent role in exploring the strong interaction dynamics of hadronic reactions in the framework of QCD. In this context one of the simplest exclusive matrix elements is the pion-photon transition form factor $F_{\gamma\pi}(Q^2)$ which appears in the process $\gamma\gamma^* \to \pi^0$. At large momentum transfer, it serves for testing theoretical predictions based upon perturbative QCD factorization.

Experimentally, the pion-photon transition form factor (TFF) with one on-shell and one off-shell photon can be extracted from measurements of the differential $e^+e^- \to e^+e^-\pi^0$ cross section [1–3]. A measurement of BaBar in 2009 [2] reported on an unexpected scaling violation of the TFF at large Q^2 (see Fig. 1) which triggered quite some interest in the community.
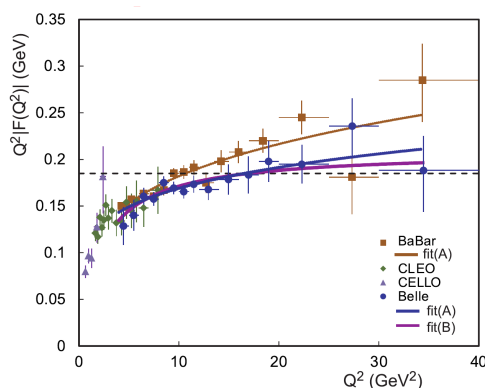
Figure 1: The $\gamma\gamma^* \to \pi^0$ transition form factor multiplied by Q^2. The dashed line indicates the asymptotic behaviour of the form factor. Taken from [3].

A subsequent analysis at Belle [3] did not find the pronounced increase of the pion TFF in the high-Q^2 region, resulting in a moderate overall tension. The large amount of data that will be accumulated at Belle II will eventually clarify the situation.

On the theory side the TFF at large momentum transfer is expanded in powers of $\Lambda^2_{\text{QCD}}/Q^2$, and at leading power (LP) it is expressed as a convolution of the perturbatively calculable hard coefficient function (CF) with the twist-two pion light-cone distribution amplitude (LCDA) in accordance with the hard-collinear factorization theorem [4]. While the hard CF has been studied to next-to-leading order (NLO) [5–8] and in the large-β_0 approximation at next-to-next-to-leading order (NNLO) [9], the full NNLO QCD correction was missing until recently, and we report on its analytic computation in the present article. The pion distribution amplitude, on the other hand, is the non-perturbative object in the factorization formula, which thanks to its universality is of great importance also for other processes such as the semileptonic or nonleptonic decays of B-mesons.

The full analytic NNLO QCD prediction of the TFF $F_{\gamma\pi}(Q^2)$ in $\gamma\gamma^* \to \pi^0$ was first put forward in [10], with a parallel computation appearing in [11] and the two results being in full agreement with each other. Our computation takes advantage of the soft-collinear effective theory (SCET) factorization program. To this end, we evaluate an appropriate bare QCD matrix element at $\mathcal{O}(\alpha_s^2)$ using modern multi-loop techniques, and implement the ultraviolet (UV) renormalization and infrared (IR) subtraction, including the proper treatment of the emerging evanescent operator, together with the subtleties arising from the γ_5 ambiguity of dimensional regularization. Furthermore, we analyse the numerical impact of the two-loop correction to the TFF, and compare different models for the twist-two pion LCDA to current experimental data. While current data still leaves room for interpretation, confronting the obtained theory predictions with the forthcoming precision of Belle II measurements will allow to distinguish between different LCDA models.

2 The pion-photon transition form factor

We start by setting up the theory framework for establishing the hard-collinear factorization formula of the transition form factor $F_{\gamma\pi}(Q^2)$, which is defined in terms of the matrix element of the electromagnetic current between an on-shell photon with momentum p' and a pion with momentum p,

$$\langle \pi(p)|j^{\text{em}}_\mu|\gamma(p')\rangle = g^2_{\text{em}}\epsilon_{\mu\nu\alpha\beta}q^\alpha p^\beta \epsilon^\nu(p')F_{\gamma\pi}(Q^2). \tag{1}$$

Here $q = p - p'$ is the transfer momentum and $Q^2 = -q^2$. $\epsilon^\nu(p')$ is the polarization vector of the on-shell photon, and e_q denotes the electric charge of the quark field in units of the positron charge. For later convenience we also introduce two light-like vectors n_μ and $\bar{n}_\mu$ satisfying $n^2 = \bar{n}^2 = 0$ and $n \cdot \bar{n} = 2$. They allow for the definition of the perpendicular component of any four-vector via $a^\mu = (n \cdot a)\bar{n}^\mu/2 + (\bar{n} \cdot a)n^\mu/2 + a_\perp^\mu$. The kinematics at leading power can then be taken as $p_\mu = (\bar{n} \cdot p)/2\, n_\mu$ and $p'_\mu = (n \cdot p')/2\, \bar{n}_\mu$, which entails the scaling $(\bar{n} \cdot p) \sim (n \cdot p') \sim \mathcal{O}(\sqrt{Q^2})$.

Applying the hard-collinear factorization theorem results in the following LP contribution to the $\gamma\gamma^* \to \pi^0$ form factor

$$F_{\gamma\pi}^{\mathrm{LP}}(Q^2) = \frac{(e_u^2 - e_d^2)f_\pi}{\sqrt{2}\,Q^2} \int_0^1 dx\, T_2(x, Q^2, \mu)\, \phi_\pi(x, \mu) \equiv \frac{(e_u^2 - e_d^2)f_\pi}{\sqrt{2}\,Q^2} T_2(x, Q^2, \mu) \otimes \phi_\pi(x, \mu). \tag{2}$$

Here T_2 is the hard coefficient function which can be expanded perturbatively in the form (similarly for any other partonic quantity)

$$T_2 = \sum_{\ell=0}^\infty a_s^\ell\, T_2^{(\ell)}, \qquad a_s \equiv \frac{\alpha_s}{4\pi}. \tag{3}$$

The non-perturbative object in the factorization formula (2) is the twist-two pion LCDA $\phi_\pi(x, \mu)$, which is defined by the renormalized matrix element on the light-cone

$$\langle \pi(p)| [\bar{q}(z\bar{n})[z\bar{n}, 0]\gamma_\mu\gamma_5 q(0)]_R |0\rangle = -if_\pi p_\mu \int_0^1 dx\, e^{ixz\bar{n}\cdot p}\, \phi_\pi(x, \mu). \tag{4}$$

$[z\bar{n}, 0]$ is the short-hand notation for the Wilson line which renders the non-local matrix element gauge invariant.

We evaluate the hard coefficient function by inspecting the following correlation function

$$\frac{g_{\mathrm{em}}^2 e_q^2}{2\,\bar{n} \cdot p} \Pi_{\mu\nu} = i \int d^4z\, e^{-iq \cdot z} \times \langle \bar{q}(\bar{x}p)q(xp)|\mathrm{T}\{j_\mu^{\mathrm{em}}(z), j_\nu^{\mathrm{em}}(0)\}|0\rangle, \tag{5}$$

which can be parameterized by the two form factors for the bilinear quark currents with the spin structures [8]

$$\Gamma_A^{\mu\nu} = \gamma_\perp^\mu \slashed{n} \gamma_\perp^\nu, \qquad\qquad \Gamma_B^{\mu\nu} = \gamma_\perp^\nu \slashed{n} \gamma_\perp^\mu. \tag{6}$$

We will devote the next section to the two-loop calculation of the bare matrix element $\Pi_{\mu\nu}^{(2)}$, and subsequently derive the master formula for the hard coefficient function T_2.

3 Two-loop calculation

The techniques that we apply during the calculation of the bare two-loop amplitude have become standard in multi-loop computations.

We generate the Feynman diagrams in two ways, with `Feynarts` [12] and by means of an in-house routine. Selected diagrams are shown in Fig. 2. The number of diagrams gets reduced by the fact that certain diagrams have color factor zero (e.g. the third one in Fig. 2), vanish due to the Furry theorem and/or represent a flavor-singlet contribution (e.g. the last one in Fig. 2). What remains is a total of 42 diagrams (plus the ones with the two photons
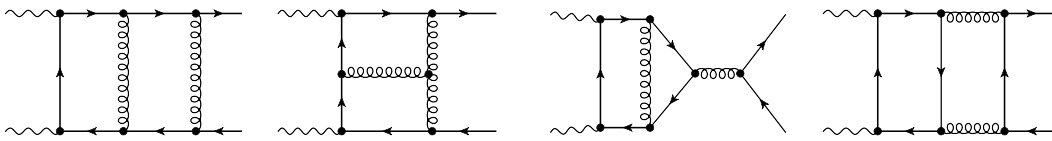
Figure 2: Sample Feynman diagrams.
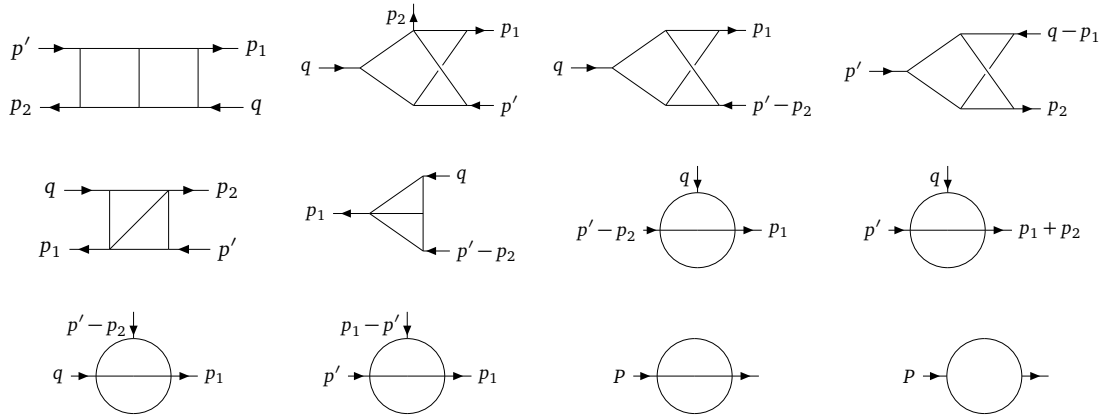
Figure 3: Complete set of master integrals for the two-loop calculation.

interchanged), which we compute using dimensional regularization with $D = 4 - 2\epsilon$ to simultaneously regulate UV and IR divergences.

After the Dirac and tensor reduction we are left with two-loop scalar integrals which we further process with the `Mathematica` version of `FIRE` [13], an implementation of Laporta's algorithm [14,15] based on integration-by-parts identities [16,17]. In addition, we exploit the fact that two of the quark momenta are parallel to each other, $p_1 \equiv xp \propto (1-x)p \equiv \bar{x}p = p_2$, which yields additional relations between integrals based on momentum conservation, which in turn enable us to arrive at the minimal set of master integrals. It is also worth mentioning that at this stage, additional Dirac structures besides $\Gamma^{\mu\nu}_{A,B}$ disappear from the sum of all diagrams, making the QED Ward identity and charge symmetry manifest and providing an important check of our calculation.

In total, we get the 12 independent master integrals depicted in Fig. 3. The easier ones among them can be solved in closed form in terms of Gamma- and hypergeometric functions, which we expand in ϵ with `HypExp` [18, 19]. The more complicated ones are evaluated with the method of differential equations [20–23], partially in a canonical basis [24]. Furthermore, Mellin-Barnes representations [25] are employed, both to compute asymptotic expansions for $x \to 0$ or $x \to 1$ to get the boundary conditions for the differential equations, and to derive the full analytic expressions of the master integrals. The sector decomposition program `FIESTA` [26,27] is used to perform numerical checks of our analytic results. We obtain the ϵ-expansion of all master integrals analytically in terms of harmonic polylogarithms (HPLs) [28–30] with weight-indices 0 and 1. To the order we are working, HPLs of at most weight four appear in the amplitude. Below, we give the results for the master integrals in the first column of Fig. 3, which we label $I_1(x)$, $I_5(x)$ and $I_9(x)$. Using $\int d^D k/(2\pi)^D$ as integration measure, and factoring out $(i/((4\pi)^{D/2}\Gamma(1-\epsilon)))^2$ together with an appropriate power of Q^2 to make the integral dimensionless, we obtain ($H_{a_1,\dots,a_n}(x)$ are HPLs)

$$\bar{x}^2 x \epsilon^4 I_1(x) = -1 + 2\epsilon(H_0(x) - H_1(x)) + \epsilon^2 \left(H_2(x) - 4H_{0,0}(x) + 3H_{1,0}(x) - 4H_{1,1}(x) - \tfrac{1}{2}\zeta_2 \right)$$

$$+ \epsilon^3 \left(\zeta_2 H_0(x) - 3\zeta_2 H_1(x) - 2H_3(x) + 2H_{1,2}(x) + H_{2,0}(x) - H_{2,1}(x) + 8H_{0,0,0}(x) \right.$$

$$-6H_{1,0,0}(x)+4H_{1,1,0}(x)-8H_{1,1,1}(x)+\tfrac{13}{2}\zeta_3\big)+\epsilon^4\big(-13\zeta_3 H_0(x)+5\zeta_3 H_1(x)$$

$$-\zeta_2 H_2(x)-2\zeta_2 H_{0,0}(x)-10\zeta_2 H_{1,1}(x)-2H_{1,3}(x)-5H_{2,1,1}(x)-2H_{2,0,0}(x)$$

$$-2H_{3,0}(x)-H_{3,1}(x)+4H_{1,1,2}(x)+4H_4(x)-H_{2,1,0}(x)-H_{2,2}(x)-8H_{1,1,0,0}(x)$$

$$-16H_{0,0,0,0}(x)+12H_{1,0,0,0}(x)+4H_{1,1,1,0}(x)-16H_{1,1,1,1}(x)\big)+\mathcal{O}(\epsilon^5), \qquad (7)$$

$$\epsilon^4 I_5(x)=\epsilon^3\big(-\zeta_2 H_0(x)-\zeta_2 H_1(x)+H_3(x)+H_{1,2}(x)-H_{2,0}(x)-H_{1,1,0}(x)+3\zeta_3\big)$$

$$+\epsilon^4\big(-7\zeta_3 H_0(x)+5\zeta_3 H_1(x)+\zeta_2 H_2(x)-2H_{1,2,0}(x)+2\zeta_2 H_{0,0}(x)-2\zeta_2 H_{1,0}(x)$$

$$-3\zeta_2 H_{1,1}(x)+H_{2,1,0}(x)-2H_{2,2}(x)+2H_{3,0}(x)+2H_{3,1}(x)+2H_{1,1,2}(x)-3H_4(x)$$

$$+2H_{1,2,1}(x)+2H_{2,0,0}(x)+H_{1,3}(x)+2H_{1,1,0,0}(x)-3H_{1,1,1,0}(x)+\tfrac{51}{4}\zeta_4\big)+\mathcal{O}(\epsilon^5), \qquad (8)$$

$$I_9(x)=\frac{\Gamma^5(1-\epsilon)\Gamma(1-2\epsilon)\Gamma(\epsilon)\Gamma(2\epsilon)}{\Gamma(2-3\epsilon)\Gamma(2-2\epsilon)\Gamma(1+\epsilon)}\,{}_2F_1(1,2\epsilon;1+\epsilon;x). \qquad (9)$$

4 UV renormalization and IR subtraction

To arrive at the two-loop contribution to $T_2(x)$ we must perform UV renormalization and IR subtraction. This is done by first introducing the basis $\{O_1^{\mu\nu}, O_2^{\mu\nu}, O_E^{\mu\nu}\}$ of non-local operators,

$$O_j^{\mu\nu}(x)=\frac{\bar{n}\cdot p}{2\pi}\int d\tau\;e^{i\bar{x}\tau\bar{n}\cdot p}\,\bar{q}(\tau\bar{n})\,[\tau\bar{n},0]\,\Gamma_j^{\mu\nu}\,q(0), \qquad (10)$$

where

$$\Gamma_1^{\mu\nu}=g_\perp^{\mu\nu}\,\slashed{n}, \qquad \Gamma_2^{\mu\nu}=i\,\epsilon_\perp^{\mu\nu}\,\slashed{n}\,\gamma_5, \qquad \Gamma_E^{\mu\nu}=\slashed{n}\left(\tfrac{1}{2}[\gamma_\perp^\mu,\gamma_\perp^\nu]-i\,\epsilon_\perp^{\mu\nu}\,\gamma_5\right), \qquad (11)$$

and then by exploiting the matching equation

$$\Pi^{\mu\nu}=\sum_{a=1,2,E}T_a\otimes\langle O_a^{\mu\nu}\rangle. \qquad (12)$$

By employing the definitions $g_\perp^{\mu\nu}=g^{\mu\nu}-n^\mu\bar{n}^\nu/2-n^\nu\bar{n}^\mu/2$ and $\epsilon_\perp^{\mu\nu}\equiv\epsilon^{\mu\nu\alpha\beta}\bar{n}_\alpha n_\beta/2$, we see that $O_E^{\mu\nu}$ is an evanescent operator, i.e. it vanishes at $D=4$. Since furthermore the CP-even operator $O_1^{\mu\nu}$ cannot couple to the pseudoscalar π^0 state, we encounter a unique physical operator $O_2^{\mu\nu}$ [8]. Moreover, the Dirac structures are related via the algebraic identities $\Gamma_{A,B}^{\mu\nu}=-(\Gamma_1^{\mu\nu}\pm\Gamma_2^{\mu\nu}\pm\Gamma_E^{\mu\nu})$ which we use to switch between different notations.

The correlator $\Pi^{\mu\nu}$ assumes the following form to all orders in α_s in terms of the tree-level matrix elements,

$$\Pi^{\mu\nu}=\sum_{k=1,2,E}\sum_{\ell=0}^\infty(Z_\alpha a_s)^\ell A_k^{(\ell)}(x)\,\langle\bar{q}(\bar{x}p)\Gamma_k^{\mu\nu}q(xp)\rangle^{(0)}, \qquad (13)$$

where the coupling renormalization factor is given by $Z_\alpha=1-a_s\beta_0/\epsilon+\mathcal{O}(a_s^2)$. Hereafter we disregard $O_1^{\mu\nu}$ completely from our consiserations due to parity. The functions T_a, $a=\{2,E\}$ are expanded as in Eq. (3). Due to scaleless integrals in dimensional regularization the matrix elements of the light-cone operators are simply expanded as

$$\langle O_a^{\mu\nu}\rangle=\sum_{\ell=0}^\infty a_s^\ell\,Z_{ab}^{(\ell)}\otimes\langle O_b^{\mu\nu}\rangle^{(0)}=\left\{\delta_{ab}+a_s Z_{ab}^{(1)}+a_s^2 Z_{ab}^{(2)}+\mathcal{O}(a_s^3)\right\}\otimes\langle O_b^{\mu\nu}\rangle^{(0)}. \qquad (14)$$

As indicated above, sums over repeated indices run over $\{2, E\}$. $\langle O_a^{\mu\nu}\rangle^{(0)}$ is the tree-level matrix element of $O_a^{\mu\nu}$, and the renormalization constants $Z_{22}^{(\ell)}$ can be extracted from the Efremov-Radyushkin-Brodsky-Lepage (ERBL) kernel [4,31–36]. Inserting Eqs. (3), (13), and (14) into Eq. (12) and comparing coefficients of $\langle O_{2,E}^{\mu\nu}\rangle^{(0)}$ at any given order in a_s, we derive the following "master formulas" for the hard CF at the various loop orders

$$T_2^{(0)} = T_E^{(0)} = A_2^{(0)},$$

$$T_2^{(1)} = A_2^{(1)} - \sum_{a=2,E} Z_{a2}^{(1)} \otimes T_a^{(0)} = T_E^{(1)} - Z_{E2}^{(1)} \otimes T_E^{(0)},$$

$$T_2^{(2)} = A_2^{(2)} + Z_\alpha^{(1)} A_2^{(1)} - \sum_{a=2,E} \sum_{k=0}^{1} Z_{a2}^{(2-k)} \otimes T_a^{(k)}. \tag{15}$$

The derivation of these formulas made further use of the relations $A_2^{(\ell)} = A_E^{(\ell)}$, $Z_{EE}^{(1)} = Z_{22}^{(1)}$ and $Z_{12}^{(1)} = Z_{2E}^{(1)} = 0$.

Finally, a word on the mixing between evanescent and physical operators is in order. The master formulas (15) were derived under the assumption that dimensional regularization is in Eq. (12) for both UV and IR divergences. However, to determine the UV-renormalization constants $Z_{ab}^{(\ell)}$ a different procedure has to be adopted. To this end, the renormalized matrix elements of the effective operators are expressed as

$$\langle O_a^{\mu\nu}\rangle = \left\{ \delta_{ab} + a_s \left[M_{ab}^{(1)} + Z_{ab}^{(1)} \right] + a_s^2 \left[M_{ab}^{(2)} + Z_{ab}^{(2)} + Z_{a2}^{(1)} \otimes M_{2b}^{(1)} \right] + \mathcal{O}(a_s^3) \right\} \otimes \langle O_b^{\mu\nu}\rangle^{(0)}, \tag{16}$$

and the matrix elements $M_{ab}^{(\ell)}$ are obtained with dimensional regularization applied only to the UV divergences but with the IR regularization scheme being different from the dimensional one, see e.g. also [8,37]. Renormalizing the matrix elements of the evanescent operator to zero yields the relations

$$Z_{E2}^{(1)} = -M_{E2}^{(1)}, \qquad\qquad Z_{E2}^{(2)} = -M_{E2}^{(2)} + M_{E2}^{(1)} \otimes M_{22}^{(1)}, \tag{17}$$

where $Z_{E2}^{(2)}$ is IR finite albeit both $M_{E2}^{(2)}$ and $M_{22}^{(1)}$ being IR divergent.

Collecting all individual pieces in (15) together, all the poles in ϵ are canceled explicitly as expected, which represents a nontrivial check for our calculation. As stated earlier, our final analytic result for the hard CF $T_2^{(2)}(x)$ agrees with that of a parallel computation [11], which uses quite a different approach based on arguments from conformal symmetry. The result for $T_2^{(2)}(x)$ is split up into three colour factors and can be expressed as

$$T_2^{(2)}(x) = \beta_0 C_F \left(\mathcal{K}_\beta^{(2)}(x)/x + \mathcal{K}_\beta^{(2)}(\bar{x})/\bar{x} \right) + C_F^2 \left(\mathcal{K}_F^{(2)}(x)/x + \mathcal{K}_F^{(2)}(\bar{x})/\bar{x} \right)$$
$$+ C_F/N_c \left(\mathcal{K}_N^{(2)}(x)/x + \mathcal{K}_N^{(2)}(\bar{x})/\bar{x} \right). \tag{18}$$

Our result for the color structure $C_F \beta_0$ agrees with the NNLO computation of the large-β_0 limit in [9]. The explicit expressions of the functions $\mathcal{K}_{\beta,F,N}^{(2)}(x)$ are too lengthy to be given explicitly here. They can be found in [10], whose arXiv repository also contains the functions in electronic form.

5   Numerical results

To facilitate our numerical analysis, certain assumptions (models) on the non-perturbative twist-two pion LCDA $\phi_\pi(x, \mu_0)$ have to be made. It is convenient to construct/constrain the
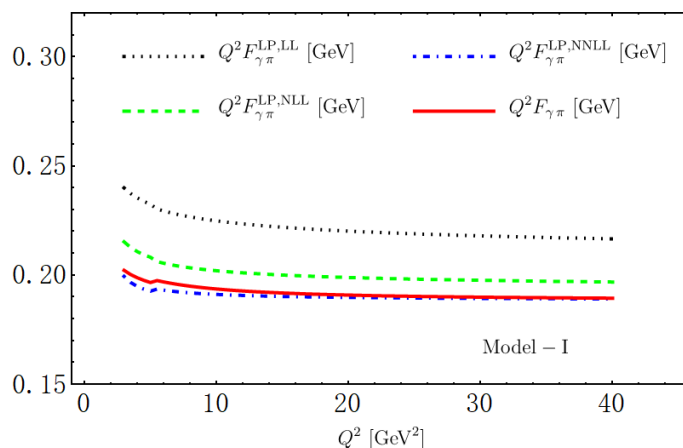
Figure 4: Theory predictions of $F_{\gamma\pi}(Q^2)$ at the LL (black dotted), NLL (green dashed), and NNLL (blue dot-dashed) order in QCD, respectively, adopting Model I in Eq. (20) as the non-perturbative input for $\phi_\pi(x, \mu_0)$. The red solid curve further includes the subleading power contributions evaluated in [8, 38].

phenomenological models via the expansion in Gegenbauer polynomials, i.e.,

$$\phi_\pi(x, \mu_0) = 6x\bar{x}\left(1 + \sum_{n=1}^{\infty} a_{2n}(\mu_0)\right) C_{2n}^{3/2}(x - \bar{x}), \tag{19}$$

where $a_{2n}(\mu_0)$ are called Gegenbauer moments. It is customary to set the reference scale $\mu_0 = 1$ GeV for model building and then evolve $\phi_\pi(x, \mu_0)$ to the proper factorization scale μ_F with the help of renormalization group equation (RGE) where the one-loop, two-loop, and three-loop ERBL evolution kernels (anomalous dimension matrix) are available in [4,31], [32–36], and [39], respectively.

As an illustration of the two-loop effect on the observable $F_{\gamma\pi}(Q^2)$, we adopt the so-called ADS/QCD model for $\phi_\pi(x, \mu_0)$ proposed in [40] with modifications from recent lattice computation of the first nontrivial Gegenbauer moment $a_2(\mu_0)$ [41] (Model I in Eq. (20) below). We display the numerical impact of QCD corrections on $F_{\gamma\pi}(Q^2)$ in Fig. 4 at leading-logarithmic order (LL), next-to-leading-logarithmic order (NLL), and next-to-next-to-leading-logarithmic order (NNLL), by including the renormalization-group evolution effect of the leading-twist pion LCDA at one loop, two loops, and three loops.

It is clear from Fig. 4 that the two-loop correction to the photon-pion TFF is rather significant. To be more specific, the NNLL correction is responsible for a $(4 \sim 7)\%$ reduction to $F_{\gamma\pi}^{\text{LP,NLL}}(Q^2)$ in the kinematic region $Q^2 \in [3, 40]$ GeV^2, in comparison to the $\sim 10\%$ reduction when advancing from $F_{\gamma\pi}^{\text{LP,LL}}$ to $F_{\gamma\pi}^{\text{LP,NLL}}$ accuracy. This pattern of QCD correction hierarchy is also observed for the other two representative models presented in Eq. (20) which validates the significance of our two-loop computation in general.

Let us now discuss the potentiality of our theory predictions in unraveling the omnipresent non-perturbative object $\phi_\pi(x, \mu)$. For this purpose, we consider three representative models,

$$\text{Model I}: \qquad \phi_\pi(x, \mu_0) = \frac{\Gamma(2 + 2\alpha_\pi)}{\Gamma^2(1 + \alpha_\pi)}(x\,\bar{x})^{\alpha_\pi}, \quad \text{with} \quad \alpha_\pi(\mu_0) = 0.422^{+0.076}_{-0.067}; \tag{20}$$

$$\text{Model II}: \qquad \{a_2, a_4, a_6, a_8\}(\mu_0) = \{0.269(47), 0.185(62), 0.141(96), 0.049(116)\};$$

$$\text{Model III}: \qquad \{a_2, a_4\}(\mu_0) = \{0.203^{+0.069}_{-0.057}, -0.143^{+0.094}_{-0.087}\}.$$
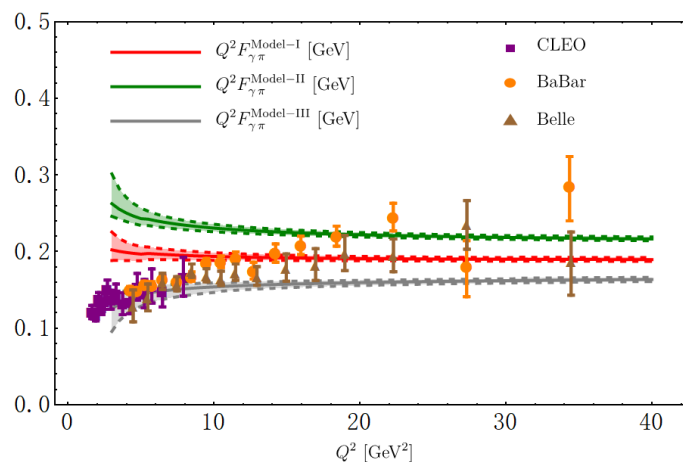
Figure 5: Theory predictions of the TFF $\gamma\gamma^* \to \pi^0$ based on the three models in (20). The color bands indicate uncertainties from factorization/renormalization scale variation $\mu_F \in [1/4, 3/4]Q^2$. For a comparison, our predictions are confronted with the experimental measurements from the CLEO [1] (purple squares), BaBar [2] (orange circles) and Belle [3] (brown spades) Collaborations.

While the background of Model I has been elaborated on above, Model II [42] and III [43–45] are proposed from the perspective of light-cone and QCD sum rules, respectively.

We collect our theory predictions of $F_{\gamma\pi}(Q^2)$ for the three models in (20) in Fig. 5, where we have purposefully neglected the error-bars quoted in Eq. (20) to enhance the characteristics of each model. It is then evident that with our two-loop correction taken into account, the perturbative uncertainties are small enough to allow to distinguish various phenomenological models for $\phi_\pi(x, \mu_0)$. As these models are formulated on vastly different principles, a concrete determination of an appropriate description for $\phi_\pi(x, \mu)$ from future experimental data will certainly be crucial to deepen our understanding of the inner structures of the hadronic states.

6 Conclusion

In conclusion, we have promoted the leading-power theory prediction of the photon-pion transition form factor to the two-loop order in QCD by combining hard-collinear factorization with modern multi-loop techniques. The analytic two-loop coefficient function we have obtained is also directly applicable in the evaluation of the axial-vector contribution to deeply virtual Compton scattering. In this article, we have presented the complete set of two-loop master integrals arising in the calculation of $\gamma\gamma^*$ annihilation into two collinear on-shell massless quarks. We expect our results to play an integral role in boosting future developments on the determination of the leading-twist pion LCDA as well as on exploring the delicate QCD dynamics of other interesting two-photon processes.

Acknowledgements

We would like to thank the authors of [11] for useful correspondence, and for sharing their analytic results with us prior to publication.

Funding information J.G. was partially supported by the Deutscher Akademischer Austauschdienst (DAAD). The research of T.H. and Y.J. was supported in part by the Deutsche Forschungsgemeinschaft (DFG, German Research Foundation) under grant 396021762 - TRR 257 ("Particle Physics Phenomenology after the Higgs Discovery") and DFG grant SFB TR 110/2. Y.M.W. acknowledges support from the National Youth Thousand Talents Program, the Youth Hundred Academic Leaders Program of Nankai University, the National Natural Science Foundation of China with Grant No. 11675082, 11735010 and 12075125, and the Natural Science Foundation of Tianjin with Grant No. 19JCJQJC61100.

References

[1] J. Gronberg et al., *Measurements of the meson-photon transition form factors of light pseudoscalar mesons at large momentum transfer*, Phys. Rev. D **57**, 33 (1998), doi:10.1103/PhysRevD.57.33.

[2] B. Aubert et al., *Measurement of the $\gamma\gamma^* \to \pi^0$ transition form factor*, Phys. Rev. D **80**, 052002 (2009), doi:10.1103/PhysRevD.80.052002.

[3] S. Uehara et al., *Measurement of $\gamma\gamma^* \to \pi^0$ transition form factor at Belle*, Phys. Rev. D **86**, 092007 (2012), doi:10.1103/PhysRevD.86.092007.

[4] G. Peter Lepage and S. J. Brodsky, *Exclusive processes in perturbative quantum chromodynamics*, Phys. Rev. D **22**, 2157 (1980), doi:10.1103/PhysRevD.22.2157.

[5] F. Del Aguila and M. K. Chase, *Higher order QCD corrections to an exclusive two-photon process*, Nucl. Phys. B **193**, 517 (1981), doi:10.1016/0550-3213(81)90344-8.

[6] E. Braaten, *Quantum-chromodynamic corrections to meson-photon transition form factors*, Phys. Rev. D **28**, 524 (1983), doi:10.1103/PhysRevD.28.524.

[7] E. P. Kadantseva, S. V. Mikhailov and A. V. Radyushkin, *Total α_s Corrections to Processes $\gamma^*\gamma^* \to \pi^0$ and $\gamma^*\pi \to \pi$ in a Perturbative QCD*, Yad. Fiz. **44**, 507 (1986).

[8] Y.-M. Wang and Y.-L. Shen, *Subleading power corrections to the pion-photon transition form factor in QCD*, J. High Energy Phys. **12**, 037 (2017), doi:10.1007/JHEP12(2017)037.

[9] B. Melić, B. Nižić and K. Passek, *Brodsky-Lepage-Mackenzie scale for the pion transition form factor*, Phys. Rev. D **65**, 053020 (2002), doi:10.1103/PhysRevD.65.053020.

[10] J. Gao, T. Huber, Y. Ji and Y.-M. Wang, *Next-to-Next-to-Leading-Order QCD Prediction for the Photon-Pion Form Factor*, Phys. Rev. Lett. **128**, 062003 (2022), doi:10.1103/PhysRevLett.128.062003.

[11] V. M. Braun, A. N. Manashov, S. Moch and J. Schönleber, *Axial-vector contributions in two-photon reactions: Pion transition form factor and deeply-virtual Compton scattering at NNLO in QCD*, Phys. Rev. D **104**, 094007 (2021), doi:10.1103/PhysRevD.104.094007.

[12] T. Hahn, *Generating Feynman diagrams and amplitudes with FeynArts 3*, Comput. Phys. Commun. **140**, 418 (2001), doi:10.1016/S0010-4655(01)00290-9.

[13] A. V. Smirnov, *Algorithm FIRE—Feynman Integral REduction*, J. High Energy Phys. **10**, 107 (2008), doi:10.1088/1126-6708/2008/10/107.

[14] S. Laporta and E. Remiddi, *The analytical value of the electron (g-2) at order α^3 in QED*, Phys. Lett. B **379**, 283 (1996), doi:10.1016/0370-2693(96)00439-X.

[15] S. Laporta, *High precision calculation of multiloop Feynman integrals by difference equations*, Int. J. Mod. Phys. A **15**, 5087 (2000), doi:10.1016/S0217-751X(00)00215-7.

[16] K. G. Chetyrkin and F. V. Tkachov, *Integration by parts: The algorithm to calculate β-functions in 4 loops*, Nucl. Phys. B **192**, 159 (1981), doi:10.1016/0550-3213(81)90199-1.

[17] F. V. Tkachov, *A theorem on analytical calculability of 4-loop renormalization group functions*, Phys. Lett. B **100**, 65 (1981), doi:10.1016/0370-2693(81)90288-4.

[18] T. Huber and D. Maître, *HypExp, a Mathematica package for expanding hypergeometric functions around integer-valued parameters*, Comput. Phys. Commun. **175**, 122 (2006), doi:10.1016/j.cpc.2006.01.007.

[19] T. Huber and D. Maître, *HypExp 2, Expanding hypergeometric functions about half-integer parameters*, Comput. Phys. Commun. **178**, 755 (2008), doi:10.1016/j.cpc.2007.12.008.

[20] A. V. Kotikov, *Differential equations method. New technique for massive Feynman diagram calculation*, Phys. Lett. B **254**, 158 (1991), doi:10.1016/0370-2693(91)90413-K.

[21] A. V. Kotikov, *Differential equation method. The calculation of N-point Feynman diagrams*, Phys. Lett. B **267**, 123 (1991), doi:10.1016/0370-2693(91)90536-Y.

[22] E. Remiddi, *Differential Equations for Feynman Graph Amplitudes*, Nuovo Cim. A **110**, 1435 (1997), arXiv:hep-th/9711188.

[23] M. Argeri and P. Mastrolia, *Feynman Diagrams and Differential Equations*, Int. J. Mod. Phys. A **22**, 4375 (2007), doi:10.1142/S0217751X07037147.

[24] J. M. Henn, *Multiloop Integrals in Dimensional Regularization Made Simple*, Phys. Rev. Lett. **110**, 251601 (2013), doi:10.1103/PhysRevLett.110.251601.

[25] M. Czakon, *Automatized analytic continuation of Mellin–Barnes integrals*, Comput. Phys. Commun. **175**, 559 (2006), doi:10.1016/j.cpc.2006.07.002.

[26] A. V. Smirnov and M. N. Tentyukov, *Feynman Integral Evaluation by a Sector decomposiTion Approach (FIESTA)*, Comput. Phys. Commun. **180**, 735 (2009), doi:10.1016/j.cpc.2008.11.006.

[27] A. V. Smirnov, *FIESTA4: Optimized Feynman integral calculations with GPU support*, Comput. Phys. Commun. **204**, 189 (2016), doi:10.1016/j.cpc.2016.03.013.

[28] E. Remiddi and J. A. M. Vermaseren, *Harmonic polylogarithms*, Int. J. Mod. Phys. A **15**, 725 (2000), doi:10.1142/S0217751X00000367.

[29] D. Maître, *HPL, a Mathematica implementation of the harmonic polylogarithms*, Comput. Phys. Commun. **174**, 222 (2006), doi:10.1016/j.cpc.2005.10.008.

[30] D. Maître, *Extension of HPL to complex arguments*, Comput. Phys. Commun. **183**, 846 (2012), doi:10.1016/j.cpc.2011.11.015.

[31] A. V. Efremov and A. V. Radyushkin, *Factorization and asymptotic behaviour of pion form factor in QCD*, Phys. Lett. B **94**, 245 (1980), doi:10.1016/0370-2693(80)90869-2.

[32] M. H. Sarmadi, *The pion evolution kernel beyond the leading order*, Phys. Lett. B **143**, 471 (1984), doi:10.1016/0370-2693(84)91504-1.

[33] F.-M. Dittes and A. V. Radyushkin, *Two-loop contribution to the evolution of the pion wave function*, Phys. Lett. B **134**, 359 (1984), doi:10.1016/0370-2693(84)90016-9.

[34] G. R. Katz, *Two-loop Feynman-gauge calculation of the meson nonsinglet evolution potential*, Phys. Rev. D **31**, 652 (1985), doi:10.1103/PhysRevD.31.652.

[35] S. V. Mikhailov and A. V. Radyushkin, *Evolution kernels in QCD: Two-loop calculation in Feynman gauge*, Nucl. Phys. B **254**, 89 (1985), doi:10.1016/0550-3213(85)90213-5.

[36] A. V. Belitsky, D. Müller and A. Freund, *Reconstruction of non-forward evolution kernels*, Phys. Lett. B **461**, 270 (1999), doi:10.1016/S0370-2693(99)00837-0.

[37] M. Beneke, T. Huber and X.-Q. Li, *NNLO vertex corrections to non-leptonic B decays: Tree amplitudes*, Nucl. Phys. B **832**, 109 (2010), doi:10.1016/j.nuclphysb.2010.02.002.

[38] A. Khodjamirian, *Form-factors of $\gamma^*\rho \to \pi$ and $\gamma^*\gamma \to \pi^0$ transitions and light cone sum rules*, Eur. Phys. J. C **6**, 477 (1999), doi:10.1007/s100520050357.

[39] V. M. Braun, A. N. Manashov, S. Moch and M. Strohmaier, *Three-loop evolution equation for flavor-nonsinglet operators in off-forward kinematics*, J. High Energy Phys. **06**, 037 (2017), doi:10.1007/JHEP06(2017)037.

[40] S. J. Brodsky and G. F. de Téramond, *Light-front dynamics and AdS/QCD correspondence: The pion form factor in the space- and time-like regions*, Phys. Rev. D **77**, 056007 (2008), doi:10.1103/PhysRevD.77.056007.

[41] G. S. Bali, V. M. Braun, S. Bürger, M. Göckeler, M. Gruber, F. Hutzler, P. Korcyl, A. Schäfer, A. Sternbeck and P. Wein, *Light-cone distribution amplitudes of pseudoscalar mesons from lattice QCD*, J. High Energy Phys. **08**, 065 (2019), doi:10.1007/JHEP08(2019)065.

[42] S. Cheng, A. Khodjamirian and A. V. Rusov, *Pion light-cone distribution amplitude from the pion electromagnetic form factor*, Phys. Rev. D **102**, 074022 (2020), doi:10.1103/PhysRevD.102.074022.

[43] A. P. Bakulev, S. V. Mikhailov and N. G. Stefanis, *QCD-based pion distribution amplitudes confronting experimental data*, Phys. Lett. B **508**, 279 (2001), doi:10.1016/S0370-2693(01)00517-2.

[44] S. V. Mikhailov, A. V. Pimikov and N. G. Stefanis, *Systematic estimation of theoretical uncertainties in the calculation of the pion-photon transition form factor using light-cone sum rules*, Phys. Rev. D **93**, 114018 (2016), doi:10.1103/PhysRevD.93.114018.

[45] N. G. Stefanis, *Pion-photon transition form factor in light cone sum rules and tests of asymptotics*, Phys. Rev. D **102**, 034022 (2020), doi:10.1103/PhysRevD.102.034022.